JOURNAL OF GEOPHYSICAL RESEARCH, VOL. 113, C02016, doi:10.1029/2007JC004371, 2008

Wind work on the geostrophic ocean circulation: An observational study of the effect of small scales in the wind stress

Chris W. Hughes[1] and Chris Wilson[1]

Received 5 June 2007; revised 3 September 2007; accepted 9 November 2007; published 20 February 2008.

[1] We use QuikSCAT scatterometer data, together with geostrophic surface currents calculated from a combination of satellite altimetry, gravity and drifter data, to investigate the rate of work done on the geostrophic circulation by wind stress. In particular, we test the suggestion that accounting for ocean currents in the calculation of stress from 10 m winds can result in a reduction of 20–35% in the wind work, compared with an approximate calculation in which currents are not accounted for. We calculate the predicted effect of accounting for ocean currents to be a reduction in power of about 0.19 TW, and find a total power input from observations which include this effect to be 0.76 TW, smaller than earlier estimates by about the right amount. By recalculating the power input using smoothed wind stresses or currents, we demonstrate that the effect of ocean currents is visible in the midlatitude data, and close to the predicted value. Proof that the data are adequate to resolve the effect in the tropics, however, is lacking, suggesting that additional processes may also be important in this region.

Citation: Hughes, C. W., and C. Wilson (2008), Wind work on the geostrophic ocean circulation: An observational study of the effect of small scales in the wind stress, *J. Geophys. Res.*, *113*, C02016, doi:10.1029/2007JC004371.

1. Introduction

[2] It is thought that the action of the wind stress on the surface geostrophic ocean flow provides power to the ocean at a rate of about 1 TW (10^{12} W). *Wunsch* [1998] used currents calculated using satellite altimetry and the EGM96 geoid [*Lemoine et al.*, 1997], together with wind stress estimated from winds (not accounting for ocean currents) from the National Centers for Environmental Prediction (NCEP), to estimate a rate of work of 0.88 TW, of which about 0.84 TW comes from the product of time-averaged wind stress and time-averaged current. The same total resulted from a model-based analysis, although with a slightly larger fractional contribution from the time-dependent term. Error estimates are difficult, but *Scott* [1999] estimated an error of 37% for the Pacific basin, on the assumption that geoid errors dominate. *Von Storch et al.* [2007] (VS hereafter) have since analyzed in some detail the power input into a 0.1° ocean model, concluding that a total of 1.1 TW is made available to the deep ocean beneath the surface boundary layer, and that Wunsch's methodology works well, leading to an estimate for this model of 1.06 TW, composed of 0.92 TW from the products of time-averaged stress and current velocity, and 0.14 TW from the time-dependent component.

[3] All of these calculations rely on the rather smooth wind stress patterns which result from numerical weather prediction models. Examination of wind stress measured by the NSCAT scatterometer, however, showed small scale structure, particularly in wind stress curl and divergence [*Milliff and Morzel*, 2001], and comparison of QuikSCAT spectra with numerical weather prediction models shows that these models strongly underestimate the power in wind stress at scales shorter than 500–1000 km [*Milliff et al.*, 2004]. In the equatorial Pacific, where strong currents and relatively weak winds occur, some of the structure in NSCAT data was seen to be due to the influence of ocean currents on wind stress [*Kelly et al.*, 2001]. Although fine structure elsewhere could not initially be clearly distinguished from sampling error, subsequent examination of longer time series from the QuikSCAT scatterometer showed a clear influence of small-scale ocean processes on the wind stress [*Chelton et al.*, 2004]. Two forms of oceanic influence are identified as being important in producing such small-scale signals [*Xie*, 2004; *Chelton et al.*, 2004]: The atmosphere-ocean temperature difference influences both the wind field and the wind stress via a quite complicated process involving the stability of, and turbulent mixing in, the marine atmospheric boundary layer. *Chelton et al.* [2004] briefly summarize the effect of small-scale temperature as a tendency to decrease the surface wind speed over cool water and increase it over warm water. The second form of influence is the ocean surface currents. Although currents are generally much slower than winds, and their effect is often neglected in wind stress formulations (which should properly be formulated in terms of the difference between wind and current velocities), currents tend to occur at shorter length scales than winds in most

[1]Proudman Oceanographic Laboratory, Liverpool, U.K.

0148-0227/08/2007JC004371$09.00

parts of the ocean, permitting this effect to stand out in differentiated measures such as wind stress curl.

[4] These observations prompted *Duhaut and Straub* [2006] (DS hereafter) to consider the implications of a link between wind stress and ocean current for calculations of the rate of wind work. Although a rather small change to the wind stress is usually implied by taking account of the current, a surprisingly large effect on the wind work (about 20%) is implied by this link. The reason is that the effect of accounting for currents is negative definite. When wind and current are in the same direction, the stress is smaller than that which would be calculated ignoring the current, and is in the same direction as the current, resulting in a smaller power input into the ocean. When they are in opposite directions, the stress is greater, but is opposing the current, reducing in an increased energy flux out of the ocean. In either case, the energy flux into the ocean is reduced. The analysis is more complicated when accounting for winds and currents in different directions but, on the assumption that the current is much slower than the wind, DS derive an equation for the error due to ignoring the current effect, which shows it to be positive definite:

$$P_1 - P = \rho_A c_d U\left(v^2 + v_0^2\right), \tag{1}$$

where P is the actual power per unit area at a particular place, P_1 is that calculated using stresses based on the wind velocity alone, ρ_A is atmospheric density, c_d is the drag coefficient (assumed constant for this derivation), U is the wind speed, v is the ocean current speed, and v_0 is the component of ocean current in the direction of the wind. A simple scaling estimate based on this formula suggests that correctly accounting for currents in calculating wind stress would result in a 20% reduction in power input to the ocean. The formula (1) refers to the instantaneous power input, and a time average involves the mean ocean surface kinetic energy (we shall see later that v_0^2 can rather accurately be replaced by $v^2/2$). As DS point out, the ocean surface kinetic energy is dominated (at least in extratropical regions) by the mesoscale, and the mesoscale in turn is dominated by the time dependent eddies and meanders, so the power reduction is expected to be strongest in regions of strong mesoscale eddy activity. From DS, an idealised numerical model experiment for a region of strong eddy activity suggests a 35% reduction (note that these percentages are all expressed relative to the larger, false estimate of power rather than the smaller, true value. A 35% reduction from false to true value is equivalent to a 54% increase of the true value to give the false value). We will call this systematic effect of currents on power the "DS effect".

[5] Model simulations have confirmed the size of this effect in more realistic geometries, for the North Pacific, where a correct wind stress formulation reduces the power input by 27% [*Dawe and Thompson*, 2006], and for an eddy-rich region of the northwest North Atlantic, where a 17% reduction occurs [*Zhai and Greatbatch*, 2007].

[6] However, none of these results are based on observations, and none include both the effects of currents and of air-sea temperature difference on wind stress. Since data are now available which allow us to map time-mean (as well as variable) currents, and wind stress, to much higher resolution than was possible for the original *Wunsch* [1998] study, this paper's aim is to provide an observational basis for this effect and an estimate of its size, together with an improved estimate of the total work done by wind on the geostrophic ocean currents.

[7] We do this in two ways, first using a (slightly extended) version of the DS formula to calculate the size of the effect to be expected by accounting for ocean currents. Secondly, we demonstrate that the effect can be seen explicitly in the observations by showing that inclusion of features in the scatterometer-measured wind stress data which occur at the oceanic mesoscale results in a reduction in power input from wind stress.

2. Description of Data

[8] We use daily wind stress measurements on a 0.25° latitude-longitude grid from 13 October 1999 to 11 October 2006 from the SeaWinds scatterometer on the QuikSCAT satellite. The instrument actually measures radar backscatter which is modified by surface ripples generated by wind stress. In other words, QuickSCAT directly measures wind stress, including the effect of ocean currents, yet is calibrated against 10 metre wind measurements [*Dunbar et al.*, 2001; *Chelton and Freilich*, 2005]. Therefore the 10 m wind is the primary high-level output of the processing, but is actually a rescaled measure of wind stress, which is subsequently calculated according to certain parameterizations. We use the *Large et al.* [1994] wind-dependent parameterisation as described in the Appendix. It is worth noting that the present (early 2007) PO.DAAC-published values of the *Large et al.* [1994] wind stress erroneously omit the factor of $\rho_A = 1.223$, resulting in an underestimate of the wind stress.

[9] We average the wind stress of the ascending pass over 7-day periods centered on the time of the altimetry in order to provide the best spatial coverage of the 4 day repeat while keeping frequencies of atmospheric variability that match the highest frequencies resolved in the altimeter product used for currents. This also fills gaps due to contamination of the scatterometer signal by precipitation (we count rain probability in excess of 30% as missing data which is typically less than 1% of points). We choose only one pass (ascending) in order to avoid spurious horizontal gradients which are present when averaging both passes over a short time.

[10] Ocean mean dynamic height is taken from the *Maximenko and Niiler* [2005] data set, which integrates information from surface drifters, satellite altimetry, surface winds and the GRACE gravity mission [*Tapley et al.*, 2003] for the period 1992 to 2002. The data are provided on a 1/2° latitude-longitude grid and bilinearly interpolated to a 1/3° Mercator grid.

[11] Time-varying sea level anomalies are obtained from 7-day repeats of combined Topex/Poseidon and ERS-1/2 satellite altimetry [*Ducet et al.*, 2000] from 13 October 1999 to 11 October 2006 on a 1/3° Mercator grid. This period is chosen to cover the largest number of whole years that coincided with the wind stress measurements.

[12] The 7-day ocean current is calculated by subtracting the time-mean of the sea level anomalies for the period 14 October 1992 to 9 October 2002 (the period used for the

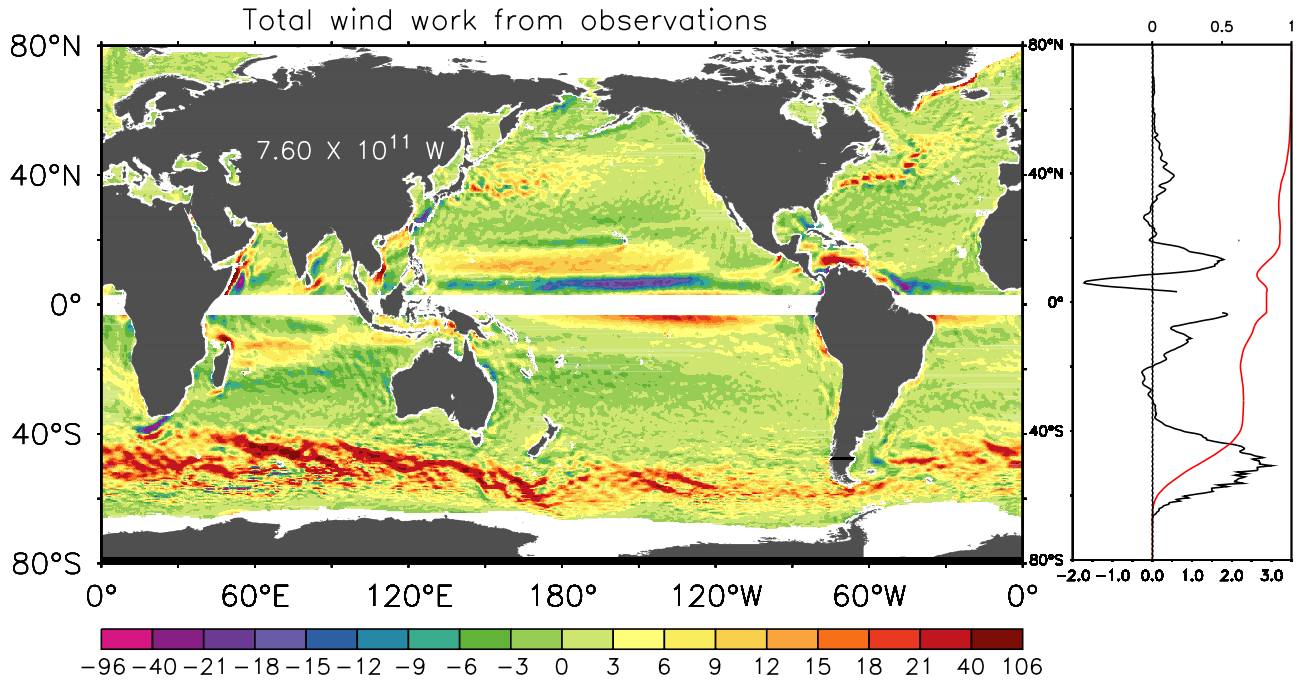

Figure 1. Wind work (10^{-3} Wm^{-2}, left), its zonal integral (10^5 Wm^{-1}, right, black), and normalized cumulative integral, starting at the southern boundary (right, red). The globally integrated value is shown in white.

mean dynamic height calculation) from the mean dynamic height and then adding the 7-day sea level anomaly back on. The daily 10 m wind is used to calculate daily wind stress, with values corrupted by rain removed. Valid values of daily wind stress which fall within the 7-day bin centered on the altimetric period were then averaged to form a 7-day mean.

[13] To calculate the power, $P = \boldsymbol{\tau} \cdot \boldsymbol{v}$, the geostrophic current is calculated using centered differences, and the 7-day wind stress is regridded to the altimetric current grid using bilinear interpolation. For time-mean quantities, we reject regions with 100 or fewer valid contributing time values (i.e., there must be valid values for more than approximately one quarter of the time.) This has most effect in regions which have seasonal ice cover.

[14] Both satellite products come with error estimates. For wind speed, the pre-launch requirements were 2 ms^{-1} RMS error for 3–20 ms^{-1} and 10% for 20–30 ms^{-1}; for wind direction it is 20° for 3–30 ms^{-1}. A post-launch assessment [*Chelton and Freilich*, 2005] suggests that the actual errors are better characterized by random component errors of 0.75 ms^{-1} along-wind and 1.5 ms^{-1} across-wind. For altimetry the error is spatially variable, but usually less than 0.04 m. We have not attempted an error estimate for the power, as this depends (as we see below) in a complicated way on both spatial and temporal correlations which cannot be accounted for without much more detailed error covariances.

3. Results

[15] The combination of scatterometer wind stress and currents from altimetry results in a total power input to the geostrophic circulation of 0.76 TW, distributed as illustrated in Figure 1. The distribution with latitude is very similar to that found by *Wunsch* [1998]: although the Southern Ocean is slightly less dominant, it still accounts for more than 60% of the total power input. Differences are greatest in the tropics, where a small Coriolis parameter means that small errors in the mean sea surface can lead to substantial errors in the geostrophic current. The spatial patterns are very similar to those seen by VS, including those in the tropics. Following Wunsch and VS, we have omitted from our calculation a band of 3° either side of the equator, because both geostrophy and the concept of an Ekman layer break down in this region. However, the power input is strong and positive either side of this gap. If we simply filled the gap by linear interpolation from north and south, we would get approximately 80 GW = 0.08 TW of extra power input from this region.

[16] The 0.76 TW power input is somewhat less than the estimates of 0.88 TW and 1.1 TW from Wunsch and from VS, respectively. The smaller value is consistent with the prediction of DS that the effect of currents should lead to a smaller power input. The reduction is 14% compared to the Wunsch estimate, and 31% compared to the VS result.

[17] How much reduction should we expect? A formula is derived in DS for the difference in power resulting from the effect of currents on wind stress, but that formula assumes a constant drag coefficient. Since the drag coefficient used in the observations is not constant, we must use a slightly generalized formula, derived in the Appendix. In short, if wind at 10 m above the ocean is $\boldsymbol{U}$, with amplitude U, and geostrophic surface current is $\boldsymbol{v}$ with amplitude v, and with component v_0 along the direction of the wind, and if the wind stress is given by $\boldsymbol{\tau} = \boldsymbol{U}F(U)$ when ignoring currents, and by $\boldsymbol{\tau} = \boldsymbol{U}_r F(U_r)$ when accounting for currents ($\boldsymbol{U}_r$ =

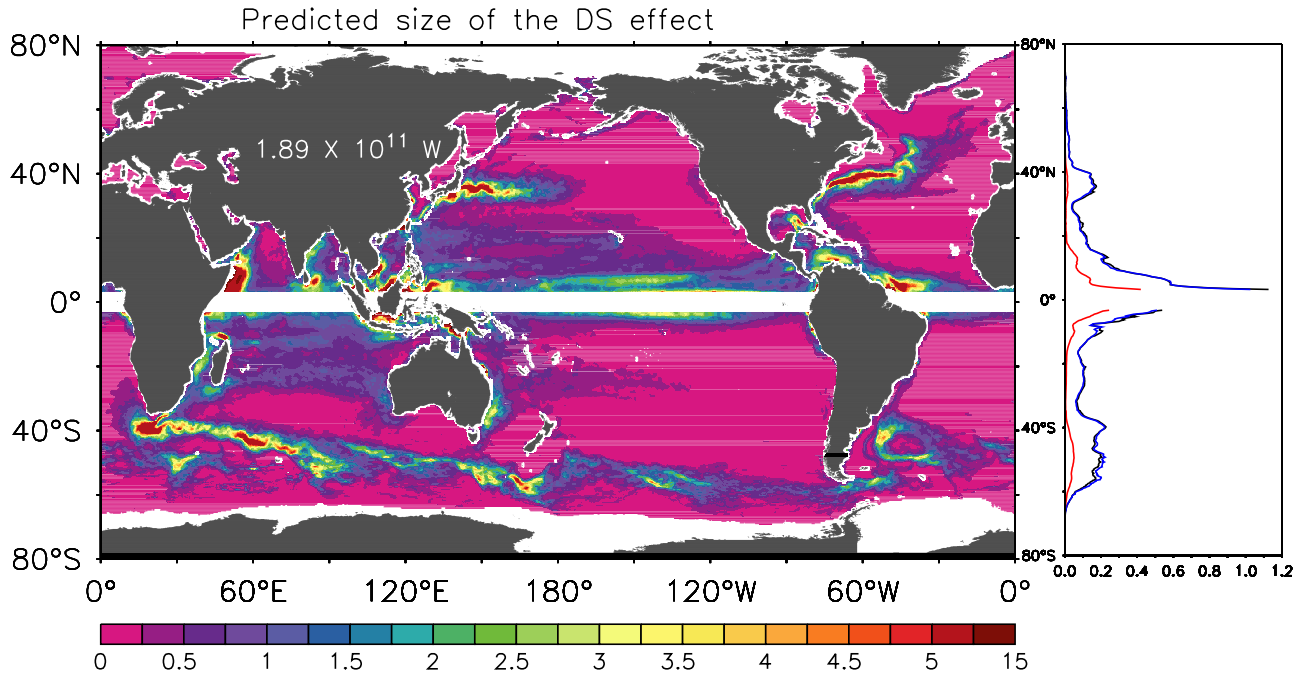

Figure 2. Increase in wind work resulting from ignoring the effect of ocean currents based on generalized DS estimate, $P_d \approx v^2\, F(U) + UF'(U)v_0^2$ (10^{-3} Wm^{-2}, left). Its zonal integral is shown in black (10^5 Wm^{-1}, right), as are those for the same estimate with 5° smoothed wind (blue) and 5° smoothed current (red).

$\boldsymbol{U} - \boldsymbol{v}$), then the increase in power resulting from ignoring the effect of currents can be written as

$$P_d = P_1 - P \approx v^2 F(U) + UF'(U)v_0^2, \tag{2}$$

where $F' = dF/dU$, and the approximation is accurate to $O(\epsilon)$ where $\epsilon = v/U$. To this order it is irrelevant whether U or U_r is used in the formula. As an estimate of the size of ϵ, we calculated the ratio of root-mean square ocean current to root-mean square wind speed. The result (not shown) is below 0.03 over a substantial fraction of the ocean, rising to about 0.07 in areas of moderate eddy activity and peaking around 0.15 in the most energetic eddy regions as well as within about 5 degrees of the equator.

[18] Given $\boldsymbol{U}$ and $\boldsymbol{v}$, we can calculate all the terms in this equation. The result is shown in Figure 2. The total difference is 189 GW (0.189 TW), and the spatial distribution is clearly associated strongly with both mean and time-dependent ocean currents. The distribution with latitude is rather different from the total power P: the tropics now dominate the large-scale integrals, accounting for more than half of the difference term, although the Antarctic Circumpolar Current, the Gulf Stream, and the Kuroshio remain important. Two other zonal integrals are plotted in Figure 2: an integral based on a calculation using spatially smoothed wind stress (using a 5° box-car filter), and an integral based on a calculation using spatially smoothed currents (the same filter). It is clear, as expected, that the small scales in the wind stress make little difference to the estimate, but that small scales in the currents are crucial.

[19] It is informative to break down the various terms in (2) to determine how important the details are. If correlations between wind and current are unimportant in the formula, then it could be approximated by

$$P_{d1} = \bar{F}\overline{v^2} + \overline{UF'}\overline{v_0^2}, \tag{3}$$

where an overline represents a time average. Furthermore, if the directions of currents and winds are not correlated, then a typical value of v_0^2 would be half of v^2, since a randomly chosen component should represent a fraction $1/\sqrt{2}$ of the total amplitude, which allows a further approximation:

$$P_{d2} = \overline{v^2}\left(\bar{F} + \overline{UF'}/2\right). \tag{4}$$

Finally, if we assume that eddy kinetic energy dominates over kinetic energy of the mean flow, then we have a third approximation:

$$P_{d3} = \overline{v'^2}\left(\bar{F} + \overline{UF'}/2\right), \tag{5}$$

where v' represents the amplitude of the difference between instantaneous current velocity and time-averaged current velocity.

[20] Zonal integrals based on the full formula, and on these three approximations, are shown in Figure 3. It is clear from these that details of the correlations are not important, and that most of P_d (more than 75%) is the result of eddy rather than mean kinetic energy. What is meant by eddy kinetic energy varies rather a lot with latitude though. As VS point out, much of the time dependence in the tropics is seasonal, whereas the midlatitude time dependence is more dominated by mesoscale eddies and meanders of the jets. It seems that a power difference estimate of about 0.19 TW is

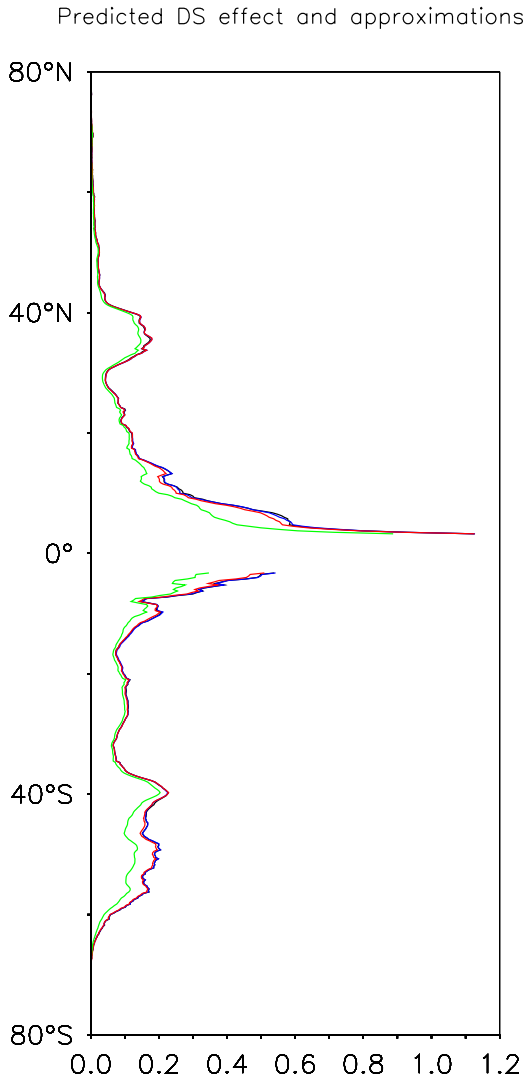

Figure 3. Zonal integral of $\overline{P_d} \approx \overline{v^2 F(U) + UF'(U)v_0^2}$ (black) and its approximations, whose relevance is described in the text: $\overline{P_{d1}} = \bar{F}\,\overline{v^2} + \overline{UF'}\,\overline{v_0^2}$ (blue), $\overline{P_{d2}} = \overline{v^2}\,(\bar{F} + \overline{UF'}/2)$ (red) and $\overline{P_{d3}} = \overline{v'^2}\,(\bar{F} + \overline{UF'}/2)$ (green) (10^5 Wm^{-1}). The black and blue lines are almost indistinguishable.

fairly robust, depending only on the amplitudes of currents and of two functions of the broad wind stress. In fact this is probably an underestimate of the effect, since increasing the resolution of the current measurements can only lead to an increase in kinetic energy (although removal of any noise from the currents would produce a decrease).

[21] Simply adding the difference of approximately 0.19 TW to the total measured value of 0.76 TW gives a total of 0.95 TW as the value which would be calculated given measurements of the winds but ignoring the effect of currents on wind stress. This lies comfortably between the Wunsch and VS estimates, which do ignore this effect. However, this simple calculation assumes that the DS effect is fully captured (to the resolution of the currents used) by the observations. There are several reasons why this might not be the case. Although the effect of ocean currents is certainly captured by the scatterometer measurements, capturing the DS effect requires that wind stress and current measurements be matched well-enough in time and space for the mesoscale features in both currents and wind stresses to be aligned. It is possible that this sampling requirement will not be met, in which case the anticorrelation between mesoscale wind stress and currents, responsible for the DS effect, will be diluted. There is also an issue of whether the DS effect is the dominant effect of the ocean mesoscale on power. *Chelton et al.* [2004] found surface temperature effects to be as important as current effects in their influence on wind stress. It is possible that these also have an integrated effect on power, although we should expect more cancellation of the temperature effect since it tends to differentiate between the warm and cold sides of a jet rather than between the jet and its surroundings as for the current effect (most extratropical jets have a warm and a cold side, although the Gulf Stream, for example, advects a tongue of warm water along its core, making the jet warmer than its surroundings: in these circumstances, a systematic temperature effect is to be expected).

[22] In order to test whether the observations do capture the DS effect, we recalculated the power input using spatially smoothed wind stress. The assumption is that this will filter out the imprint of mesoscale ocean processes on the wind stress, thus removing most of the DS effect, although the part of the DS effect which is due to larger-scale ocean currents will remain. Smoothing the currents rather than wind stress achieves the same effect, and produces very similar integral values. Note, however, that we cannot distinguish here between mesoscale effects due to currents and those due to sea surface temperature.

[23] Each 7-day average wind stress field from the scatterometer was subjected to a 3°, 5° or 10° box-car smoothing before taking the product with the current (smoothing is performed on a Mercator grid, so that the smoother is 3°, 5° or 10° in longitude, and the same distance in km in latitude, giving a square smoothing region). The effect of this smoothing is to reduce the strength of the wind stress slightly, since a part of the true 10 m wind is filtered out by this smoothing (large-scale averages of the reduction in time-averaged wind stress strength for 5° smoothing are around 5–15%, part of which is due to the DS effect and part due to the smoothing of the winds themselves; the reduction is smallest in the tropics), and to filter out the part of the wind stress which is associated with small-scale oceanic processes. Despite the reduction in wind stress, the effect of this smoothing is to increase the power into the ocean, by about 49 GW with 3° smoothing and by 60 GW with 5° smoothing, although the effect begins to decrease with 10° smoothing which leads to only a 26 GW increase as the winds are damped out more strongly by this degree of smoothing. The spatial distribution of the difference resulting from 5° smoothing is shown in Figure 4. As expected from DS, the midlatitude power increase is strongest where the surface kinetic energy is greatest. The effect is, however, much weaker than expected in the tropics.

[24] Another feature which is apparent in Figure 4 is the appearance of dipoles across a number of jets. This is clearest for the Gulf Stream, the tips of Madagascar, and a number of topographically steered jets in the Antarctic Circumpolar Current. If the DS effect was the only effect of the ocean mesoscale on wind stress, then we would expect the values in Figure 4 to be everywhere positive. In

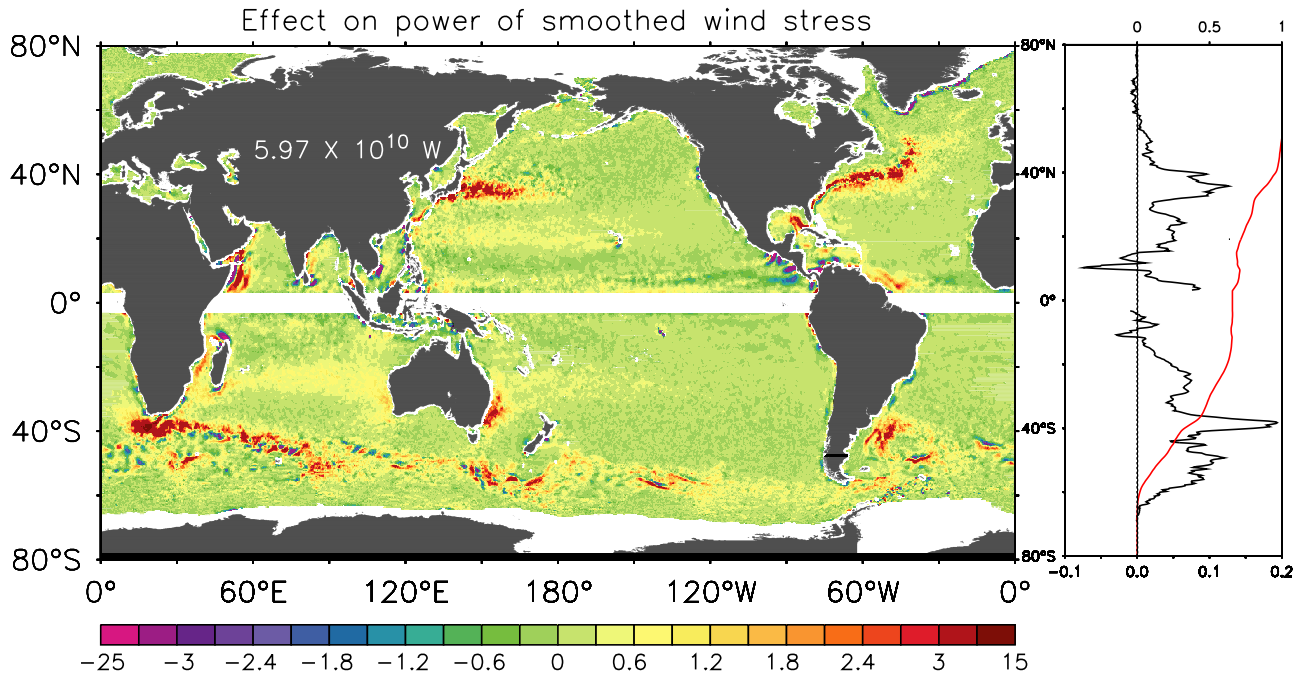

Figure 4. Increase in wind work when wind stress is smoothed by 5° $\overline{\tau_{sm5} \cdot v} - \overline{\tau \cdot v}$ (10^{-3} Wm^{-2}, left), its zonal integral (10^5 Wm^{-1}, right, black), and normalized cumulative integral, starting at the southern boundary (right, red).

fact, the dipole regions are consistent with the influence of sea surface temperature. When the wind and jet are both (roughly) eastward, as in the midlatitude regions, there is a larger wind stress on the warm (equatorward) side and a smaller wind stress on the cold (poleward) side of the jet. This produces a reduction of power into the ocean on the poleward side of the jet, and an increase on the equatorward side. Since the effect of the mesoscale is the negative of the quantity plotted in Figure 4, the signs of the dipoles are consistent with this interpretation.

[25] Using smoothed wind stress is not a perfect way of assessing the DS effect, since it does not remove all of the effect of ocean currents on wind stress (not all currents integrate to zero over a 5° box), and it removes some fine scales which may be due to winds. An independent check can be made in regions dominated by mesoscale eddies by considering the time-dependent component of the power input, i.e., by looking at the term $\overline{\tau' \cdot v'} = \overline{\tau \cdot v} - \bar{\tau} \cdot \bar{v}$, where an overline represents a time average, and prime represents deviations from the time average. The reason for examining this quantity is that, if winds and currents are uncorrelated in time, then the covariance between wind stress and current represents the DS effect resulting from the time-dependent part of the current. As noted above, this represents more than 75% of the total DS effect. Of course it is not always true that winds and currents are uncorrelated, indeed many currents are wind-driven, and in these regions we would expect $\overline{\tau' \cdot v'}$ to be positive. This is the case in the diagnostics of *Wunsch* [1998] and VS, who find a positive global integral of this term (39 GW for the Wunsch observations, about 65 GW for the model considered by Wunsch, and 140 GW for VS). However, where the time-dependent current is dominated by more stochastic mesoscale eddies and meanders, the result of intrinsic instability processes rather than direct atmospheric forcing, the DS effect should dominate and the term should become negative.

[26] Figure 5a shows this time-dependent term. At first glance, the result looks very similar to Figure 2 of VS. Strong positive and negative contributions occur in the tropics, with the positive contribution (representing wind-driven currents) dominating. A positive contribution similarly predominates around many continental margins, again indicative of wind-driven currents (although the temperature effect may also be important here, as wind stress is also correlated with temperature signals via upwelling in many regions). The regions of strong mesoscale variability show very patchy power distributions, as in VS. Closer inspection, however, shows that there is a bias to negative contributions in these regions, which shows clearly in the zonal integrals. This is even more clear in Figure 5b, which is the same as Figure 5a, but with a 5° smoother applied. It is now very clear that the term is negative in regions dominated by mesoscale variability.

[27] While the total value of $\overline{\tau' \cdot v'}$ remains positive, it is a very small 9.3 GW. This represents a cancellation between the effects of wind-driven currents and the DS effect, with the DS effect dominating in midlatitudes and wind-driven currents dominating in the tropics. The integral between 20°S and 20°N is 39 GW, equal to Wunsch's global integral. Wunsch's calculation (his Figure 3) does show negative values in the Southern Ocean, but these are not associated with regions of mesoscale variablity and are not seen by VS. A re-examination of the data used shows unusual currents along the ice edge. A likely reason for the negative values is thus a problem with the flagging of ice when using the altimeter data (C. Wunsch, personal communication, 2007). As the negative band is partially offset by a nearby erroneous

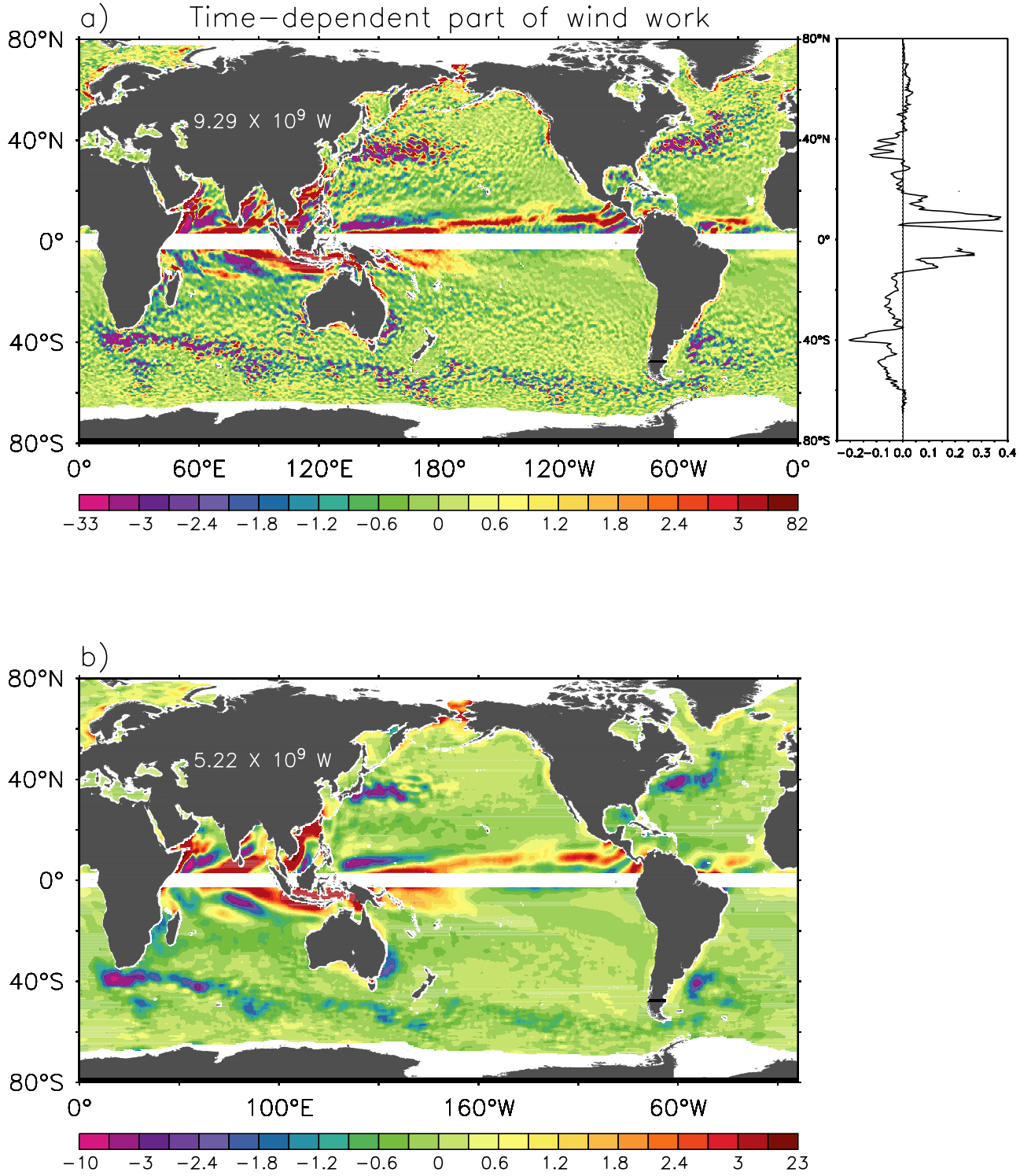

Figure 5. a) Time-dependent component of wind work, $\overline{\tau' \cdot v'}$ (10^{-3} Wm^{-2}, left) and its zonal integral (10^{5} Wm^{-1}, right). b) The same component with 5° post-smoothing (10^{-3} Wm^{-2}).

positive band, this only contributes a small effect (less than 2 GW) to the total.

[28] We thus have clear evidence that the combined sampling of altimetry and scatterometer data are sufficient to capture the DS effect in midlatitude regions, especially where the currents are dominated by mesoscale variability. The evidence is much less clear in the tropics. We quantify this in Figure 6a, in which we superimpose zonal integrals of various measures of the DS effect on power. The black curve represents a DS-based prediction of the effect we should see from ocean currents on scales smaller than 5°. This is produced by using the full DS prediction (black line

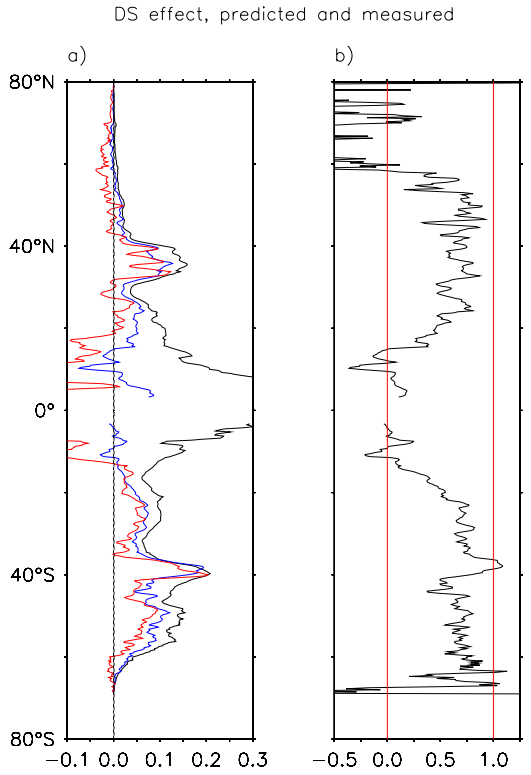

Figure 6. a) Zonal integrals of the DS effect on power (10^5 Wm^{-1}): DS-based prediction of the effect we should see by applying 5° smoothing to the wind stress (black), produced by subtracting the DS prediction based on 5°-smoothed currents (red line in Figure 2) from the full DS prediction (black line in Figure 2); the actual effect of applying 5° smoothing to the wind stress (blue), as in Figure 4; the negative of the time-dependent power component (i.e., $-\overline{\tau' \cdot v'}$) (red). b) The ratio of the actual effect of applying 5° smoothing to the wind stress to the DS-based prediction of the effect we should see by applying 5° smoothing to the wind stress (black).

in Figure 2), and subtracting from it the DS prediction based on 5°-smoothed currents (red line in Figure 2). In blue, we have the actual effect of applying 5° smoothing to the wind stress (as in Figure 4), and in red we have the negative of the time-dependent term shown in Figure 5a (i.e., $-\overline{\tau' \cdot v'}$). In midlatitude regions, the observed effect of smoothing the wind stress comes close to the DS-based prediction (typically 75%, as seen from the ratio plotted in Figure 6b). The time-dependent term captures a slightly smaller DS effect in these mesoscale-dominated regions, as expected.

[29] This high percentage at midlatitudes, despite the fact that smoothing the wind stress also removes a part of the wind effect on wind stress as well as part of the current effect, and despite the imperfectly matched sampling of the scatterometer and altimeter, clearly demonstrates that the DS effect is operating at midlatitudes, and that the combination of scatterometer and altimeter data is capturing most of this effect. This makes the discrepancy in the tropics all the more surprising.

[30] We have been unable to identify a clear reason for this difference in the tropics. Figure 4 does show strong negative contributions close to central America, which relate to small-scale patterns in wind stress which are associated with topographic steering of the winds rather than with ocean influences [*Chelton et al.*, 2004], but excising this area from the calculation only leads to an increase of about 2 GW. Winds in the tropics do not seem to be more strongly affected than elsewhere by 5° smoothing (the opposite, in fact), and strong positive tropical regions in Figure 4 seem to match quite well with the DS-based predictions in Figure 2. The main tropical reduction appears from Figure 4 to come from a broad band of moderate negative values occurring in the open ocean.

[31] Having said this, our method suffers from more complications in the tropics than elsewhere. There is not such a great separation in scales between ocean currents and atmospheric winds, the winds and currents are strongly correlated in space and time, there is a strong seasonal cycle, rapid ocean adjustment processes in this region may mean that the sampling mismatch between instruments is a more acute problem, and the region is close to the band in which geostrophic flow is masked out on approaching the equator, which complicates the effect of smoothing and increases the noise from the altimeter measurements. It is possible that our failure to confirm the DS effect in the tropics is a result of not properly accounting for these complications.

[32] The broad negative bands seen in Figure 4, however, suggest that this may be a real effect. Given the importance of seasonal cycles in this region, and the different relationship between currents and sea surface temperature from that seen in the mesoscale-dominated midlatitudes, one possibility is that the DS effect in this region is masked by the effect of ocean-atmosphere temperature difference on wind stress, which may correlate more strongly with currents here than elsewhere. Resolution of these issues will require further studies which are beyond the scope of the present work.

[33] In conclusion, we can clearly see the DS effect at work in midlatitudes, as a result of which the total power calculated from a combination of altimetry and scatterometer data is smaller than it would otherwise be. We cannot, however, clearly demonstrate whether or not the DS effect in the tropics has been properly accounted for by these measurements. The effect of currents is certainly accounted for in the scatterometer data, but we have no clear demonstration that the necessary matching of sampling between scatterometer and altimeter data has been achieved in this region.

4. Summary and Conclusions

[34] We summarize in Table 1 the various power inputs and contributions to power input calculated in this work, giving global integrals and values integrated over a Southern latitude range 80°S–20°S, a Tropical range 20°S–20°N (excluding 3°S–3°N), and a Northern range 20°N–80°N.

[35] The headline figure is a global total of 760 GW (0.76 TW), calculated by taking the time-mean dot product of scatterometer-derived wind stress and surface geostrophic currents from satellite altimetry. This is smaller than the values calculated by *Wunsch* [1998] and VS, but the large contribution of the Southern Ocean is still apparent, with the

Table 1. Power Inputs (GW) to the Global Ocean (80°S–80°N, Excluding the Equatorial Band 3°S–3°N), and Their Differences, Based on the Methods Described in the Text, and the Values Split by Region Into Southern (South of 20°S), Tropical (20°S–20°N, Excluding the Equatorial Band), and Northern (North of 20°N) Regions

Power in GW	Global	Southern	Tropical	Northern
a) $\overline{\boldsymbol{\tau} \cdot \boldsymbol{v}}$	760	481	214	64.2
b) 3° smoothed $\boldsymbol{\tau}$	809	510	221	77.3
c) 5° smoothed $\boldsymbol{\tau}$	820	518	220	80.7
d) 5° smoothed $\boldsymbol{v}$	819	520	219	79.9
e) 10° smoothed $\boldsymbol{\tau}$	786	530	182	73.9
f)10° smoothed $\boldsymbol{v}$	799	517	204	77.6
g) difference c)-a)	**60**	**37**	**6**	**16.5**
h) $\overline{\boldsymbol{\tau}' \cdot \boldsymbol{v}'}$	9.29	−25.7	39.0	−4.06
i) $\boldsymbol{P}_d$ from DS	189	62.6	96.2	29.8
j) DS P_d 5° smoothed $\boldsymbol{v}$	39.9	10.6	26.3	3.07
k) difference i)-j)	**149**	**52.0**	**69.9**	**26.7**
l) DS P_d approx. 1	189	62.4	96.4	30.0
m) DS P_d approx. 2	183	61.2	92.3	30.0
n) DS P_d approx. 3	145	48.3	71.6	25.5

Southern region accounting for more than 60% of the total power.

[36] Rather counterintuitively, if we recalculate this power input using smoothed wind stresses (or smoothed currents), the total power into the ocean apparently increases. This is in fact in line with the predictions of DS, who showed that accounting for surface currents in the calculation of wind stress results in a significant reduction in power compared to the case in which the current is not accounted for (the latter case being approximated by our smoothed wind stresses). The total power increase based on 5° smoothing is 60 GW.

[37] We derived a slight generalization of a formula due to DS which makes it possible to calculate the expected size of the DS effect using a more realistic form for the drag coefficient. This led to a predicted total of 189 GW, which reduces to 149 GW if the effect of currents on scales larger than 5° is excluded. The observed effect of 60 GW is 40% of this. We showed that the DS calculation is robust, and does not depend strongly on details of correlations between the terms involved, or on small-scale features in the winds used.

[38] Looking at the way in which these results vary with latitude reveals an interesting picture. In the Southern region the apparent power continues to increase even as the effective resolution of the wind stress is reduced by up to 10° smoothing. In the Northern region, it increases up to 5° smoothing, but decreases (although remaining higher than the unsmoothed case) with 10° smoothing, and in the Tropical region 3° smoothing produces the greatest (but still small) increase, with 10° smoothing producing a decrease compared with the unsmoothed case. This is in contrast to the DS prediction, which predicts the largest effect in the Tropical region. As a result, the observations based on 5° smoothing of wind stress capture 71% of the predicted DS effect in the Southern region, 62% in the Northern region, but only 9% in the Tropical region. The distribution of the time dependent term $\overline{\boldsymbol{\tau}' \cdot \boldsymbol{v}'}$ is also consistent with expectations of the DS effect in regions dominated by mesoscale variability.

[39] Given that the measured power decreases as the resolution of wind stress measurements increases (as expected from DS), it is safe to conclude that the total power would be less than 760 GW given perfect resolution and perfectly matched sampling. As the DS effect is clearly evident in these observations in the Northern and Southern regions, we would expect a calculation based on the same currents, but on wind stresses derived by ignoring ocean currents, to produce values at least 92 GW larger (the combination of DS predictions for Northern and Southern regions), giving at least 852 GW. If the reason for our inability to detect the DS effect in the Tropical region is, as we suspect, that there are other ocean influences on wind stress in this region which counteract the DS effect, then we can also say that we have accounted for the DS effect in the Tropical observations, and that a calculation based on wind stresses which ignore ocean currents would result in an increase of power by the full DS prediction of 189 GW, to 949 GW.

[40] These values lie close to those found by *Wunsch* [1998], from both a coarse resolution observational study and a model-based calculation, but are still below the value of 1.1 TW found in another model study by VS. It is not clear why VS found such a large value, but one place to look might be the Southern Ocean. This is a region which is notoriously difficult to model well, and is the dominant region for power input. Indeed, *Wunsch* [1998] noted that the main difference between his observational and model-based estimates was that the Southern Ocean peak in the model-based estimate was significantly smaller. This is surprising, given that the model concerned [*Semtner and Chervin*, 1992] produced a rather large circumpolar transport of about 200 Sv. Equally, the Southern Ocean might be a good place to look for errors in the mean flow used in this observational study, especially as the drifter data used are more prone to systematic effects due to winds and waves here than elsewhere [*Niiler et al.*, 2003]. However, the use of a combination of altimetry and satellite gravity data to constrain the large scales should greatly reduce this source of error in the data set used here [*Maximenko and Niiler*, 2005].

[41] To summarize, subject to unknown systematic errors in the data sets used, we find that 760 GW is an upper limit on the power input to the geostrophic ocean circulation by wind stress. We would expect a calculation which ignores the DS effect to produce a larger power of between about 850 and 950 GW (the larger number being the case if, as we suspect, the DS effect in the Tropical region is accounted for in our calculation, but masked in our diagnostics by other effects). We find clear evidence for the operation of the DS effect in midlatitude regions, but the picture appears to be more complicated in the tropics.

Appendix A

[42] DS derived a formula (their equation (A1)) for the excess power apparently input into the ocean as a result of ignoring the ocean current in the formulation for wind stress. In our notation, this formula is given in the Introduction as (1). This was derived by assuming a constant drag coefficient, and by neglecting terms which are smaller

by a factor of order $\epsilon = v/U$. It is clear that this power excess is positive definite.

[43] For our calculation using scatterometer data, we use the *Large et al.* [1994] formula for the drag coefficient: $\rho_A c_d = \alpha/U + \beta + \gamma U$, where $\alpha = 0.00270\rho_A$, $\beta = 0.000142\rho_A$, and $\gamma = 0.0000764\rho_A$, with $\rho_A = 1.223$ following the usage in scatterometer processing (all numerical values are for S.I. units). This allows us to write the wind stress as

$$\boldsymbol{\tau} = \boldsymbol{U}_r F(U_r), \tag{A1}$$

where $\boldsymbol{U}_r = \boldsymbol{U} - \boldsymbol{v}$ is the difference between 10 m wind and ocean current, and the approximate stress ignoring the ocean current is then

$$\boldsymbol{\tau}_1 = \boldsymbol{U} F(U), \tag{A2}$$

with $\boldsymbol{F}(U) = \alpha + \beta U + \gamma U^2$. The approximation used by DS is equivalent to setting $\alpha = \gamma = 0$.

[44] We wish to derive an equivalent to (1), but using the more complicated wind stress formulation. We start with

$$P_1 - P = (\boldsymbol{\tau}_1 - \boldsymbol{\tau}) \cdot \boldsymbol{v} = (F(U) - F(U_r))\boldsymbol{U} \cdot \boldsymbol{v} + v^2 F(U_r). \tag{A3}$$

We then note that $\boldsymbol{F}(U) - F(U_r) = F'(U_r)(U - U_r)(1 + O(\epsilon))$, where $F'(U_r) = dF/dU_r$, and that $U - U_r = v_0(1 + O(\epsilon))$ (recalling that v_0 is the component of $\boldsymbol{v}$ along the direction of $\boldsymbol{U}$, so that $\boldsymbol{U} \cdot \boldsymbol{v} = U v_0$). Substituting these then gives

$$P_1 - P = v^2 F(U_r) + U F'(U_r) v_0^2 (1 + O(\epsilon)). \tag{A4}$$

Neglecting the $O(\epsilon)$ term, and noting that $U = U_r(1 + O(\epsilon))$, we have

$$P_1 - P \approx v^2 F(U) + U F'(U) v_0^2, \tag{A5}$$

which can equally well be written in terms of U_r, to the same order of accuracy.

[45] When $\alpha = \gamma = 0$, $UF'(U) = F(U)$, and this reduces to the DS formula. This generalized formula is positive definite as long as $F'(U)$ is positive, which it is for the form of F considered here and for other reasonable forms, although it is possible that it becomes negative at wind speeds of around 40 ms^{-1} [*Jarosz et al.*, 2007].

[46] **Acknowledgments.** Thanks to Carl Wunsch, Rob Scott and David Straub for useful discussions and data exchange, to PO.DAAC and CLS for making the scatterometer and altimeter data available, and to Nikolai Maximenko for the mean dynamic topography. This study was funded by the UK Natural Environment Research Council, and represents a contribution to Oceans2025 Theme 1: Climate, Ocean Circulation and Sea Level.

References

Chelton, D. B., M. G. Schlax, M. H. Freilich, and R. F. Milliff (2004), Satellite measurements reveal persistent small-scale features in ocean winds, *Science*, *303*, 978–983.

Chelton, D. B., and M. H. Freilich (2005), Scatterometer-based assessment of 10 m wind analyses from the operational ECMWF and NCEP numerical weather prediction models, *Month. Weather Rev.*, *133*, 409–429.

Dawe, J. T., and L. Thompson (2006), Effect of ocean surface currents on wind stress, heat flux, and wind power input to the ocean, *Geophys. Res. Lett.*, *33*, L09604, doi:10.1029/2006GL025784.

Ducet, N., P.-Y. Le Traon, and G. Reverdin (2000), Global high resolution mapping of ocean circulation from TOPEX/Poseidon and ERS-1/2, *J. Geophys. Res.*, *105*, 19,477–19,498.

Duhaut, T. H. A., and D. N. Straub (2006), Wind stress dependence on ocean surface velocity: Implications for mechanical energy input to ocean circulation, *J. Phys. Oceanogr.*, *36*, 202–211.

Dunbar, R. S., S. V. Hsiao, Y.-J. Kim, K. S. Pak, B. H. Weiss, and A. Zhang (2001), Science algorithm specification for SeaWinds on QuikSCAT and SeaWinds on ADEOS-II, JPL Document D-21978, Jet Propulsion Laboratory, Pasadena, CA.

Jarosz, E., D. A. Mitchell, D. W. Wang, and W. J. Teague (2007), Bottom-up determination of air-sea momentum exchange under a major tropical cyclone, *Science*, *315*, 1707–1709.

Kelly, K. A., S. Dickinson, M. J. McPhaden, and G. C. Johnson (2001), Ocean currents evident in satellite wind data, *Geophys. Res. Lett.*, *28*, 2469–2472.

Large, W. G., J. C. McWilliams, and S. C. Doney (1994), Oceanic vertical mixing: A review and a model with a nonlocal boundary layer parameterization, *Rev. Geophys.*, *32*, 363–403.

Lemoine, F., et al. (1997), The development of the NASA GSFC and NIMA Joint Geopotential Model, *Proc. Int. Symp. Gravity, Geoid and Marine Geodesy*, IAG Symposium Vol. 117, edited by H. Fujimoto, Springer-Verlag, 461–469.

Maximenko, N. A., and P. P. Niiler (2005), Hybrid decade-mean global sea level with mesoscale resolution, In *Recent Advances in Marine Science and Technology*, N. Saxena (Ed.), pp. 55–59, Honolulu: PACON International.

Milliff, R. F., and J. Morzel (2001), The global distribution of the time-average wind stress curl from NSCAT, *J. Atmos. Sci.*, *58*, 109–131.

Milliff, R. F., J. Morzel, D. B. Chelton, and M. H. Freilich (2004), Wind stress curl and wind stress divergence biases from rain effects on QSCAT surface wind retrievals, *J. Atmos. Ocean. Tech.*, *21*, 1216–1231.

Niiler, P. P., N. A. Maximenko, and J. C. McWilliams (2003), Dynamically balanced absolute sea level of the global ocean derived from near-surface velocity observations, *Geophys. Res. Lett.*, *30*(22), 2164, doi:10.1029/2003GL018628.

Scott, R. B. (1999), Mechanical energy flux to the surface geostrophic flow using TOPEX/Poseidon data, *Phys. Chem. Earth Part A Solid Earth Geod.*, *24*, 399–402.

Semtner, A. J., Jr., and R. M. Chervin (1992), Ocean general circulation from a global eddy-resolving model, *J. Geophys. Res.*, *97*, 5493–5550.

Tapley, B. D., D. P. Chambers, S. Bettadpur, and J. C. Ries (2003), Large scale ocean circulation from the GRACE GGM01 Geoid, *Geophys. Res. Lett.*, *30*(22), 2163, doi:10.1029/2003GL018622.

Von Storch, J.-S., H. Sasaki, and J. Marotzke (2007), Wind-generated power input to the deep ocean: An estimate using a $\frac{1}{10}^\circ$ ocean general circulation model, *J. Phys. Oceanogr.*, *37*, 657–672.

Wunsch, C. (1998), The work done by the wind on the oceanic general circulation, *J. Phys. Oceanogr.*, *28*, 2332–2340.

Xie, S. P. (2004), Satellite observations of cool ocean-atmosphere interaction, *Bull. Amer. Met. Soc.*, 85, 195–208.

Zhai, X., and R. J. Greatbatch (2007), Wind work in a model of the northwest Atlantic Ocean, *Geophys. Res. Lett.*, *34*, L04606, doi:10.1029/2006GL028907.

Chris W. Hughes and Chris Wilson, Proudman Oceanographic Laboratory, 6 Brownlow St., Liverpool L3 5DA, U.K. (cwh@pol.ac.uk; cwi@pol.ac.uk)